



LAWRENCE  
LIVERMORE  
NATIONAL  
LABORATORY

# High-Speed, Temperature Programmable Gas Chromatography Utilizing a Microfabricated Chip with an Improved Carbon Nanotube Stationary Phase

Michael Stadermann, Olgica Bakajin, Vanessa  
Reid, Rob Synovec

August 22, 2008

Talanta

## **Disclaimer**

---

This document was prepared as an account of work sponsored by an agency of the United States government. Neither the United States government nor Lawrence Livermore National Security, LLC, nor any of their employees makes any warranty, expressed or implied, or assumes any legal liability or responsibility for the accuracy, completeness, or usefulness of any information, apparatus, product, or process disclosed, or represents that its use would not infringe privately owned rights. Reference herein to any specific commercial product, process, or service by trade name, trademark, manufacturer, or otherwise does not necessarily constitute or imply its endorsement, recommendation, or favoring by the United States government or Lawrence Livermore National Security, LLC. The views and opinions of authors expressed herein do not necessarily state or reflect those of the United States government or Lawrence Livermore National Security, LLC, and shall not be used for advertising or product endorsement purposes.

**High-Speed, Temperature Programmable Gas Chromatography Utilizing a  
Microfabricated Chip with an Improved Carbon Nanotube Stationary Phase**

Vanessa R. Reid<sup>†</sup>, Michael Stadermann<sup>‡</sup>, Olgica Bakajin<sup>‡</sup> and Robert E. Synovec<sup>†\*</sup>

<sup>†</sup>Department of Chemistry, Box 351700  
University of Washington  
Seattle, Washington 98195-1700, USA

<sup>‡</sup>Chemistry & Material Science  
Lawrence Livermore National Laboratory  
Livermore, CA 94550

\* Corresponding Author  
Fax: (+1) (206) 685-8665  
Email: [synovec@chem.washington.edu](mailto:synovec@chem.washington.edu)

Manuscript prepared for submission to *TALANTA*

July 10, 2008

## Abstract

A new growth recipe for producing single-walled carbon nanotubes (SWCNTs) combined with a new bonding technique was implemented in a microfabricated gas chromatography (micro-GC) chip. Specifically, the micro-GC chip contained a 30 cm (length) microfabricated channel with a 50  $\mu\text{m}$  x 50  $\mu\text{m}$  square cross-section. A SWCNT stationary phase “mat” was grown on the bottom of the separation channel prior to the chip bonding. Injections onto the micro-GC chip were made using a previously reported high-speed diaphragm valve technique. A FID was used for detection with a high-speed electrometer board. All together, the result was a highly efficiency, temperature programmable (via low thermal mass, rapid on-chip resistive heating) micro-GC chip. In general, the newly designed micro-GC chip can be operated at significantly lower temperature and pressure than our previously reported micro-GC chip, while producing excellent chemical separations with significantly smaller reduced plate heights,  $h$ . Scanning electron microscopy (SEM) images show a relatively thin and uniform mat of nanotubes with a thickness of  $\sim 800$  nm inside the channel. The stationary phase was further characterized using Raman spectroscopy. The uniformity of the stationary phase resulted in better separation efficiency and peak symmetry (as compared to our previous report) in the separation of a mixture of five  $n$ -alkanes ( $n$ -hexane,  $n$ -octane,  $n$ -nonane,  $n$ -decane and  $n$ -undecane). The on-chip resistive heater employing a temperature programming rate of 26  $^{\circ}\text{C}/\text{s}$  produced a peak capacity of eight within a 1.4 s time window. As a direct consequence of the stationary phase improvement, a  $\sim 5$ -fold improvement in reduced plate height,  $h$ , relative to our previous report was observed.

**Keywords:** gas chromatography, carbon nanotubes, microfabricated, high-speed, resistively heated

## 1. Introduction

Single and multi-wall carbon nanotube stationary phases for use in gas chromatography (GC) have been the subject of several recent reports [1-6]. The majority of these reports utilized carbon nanotubes within a silica capillary. Multi-walled carbon nanotubes (MWCNTs) utilized as a GC stationary phase have faster mass transfer properties than graphitic carbon stationary phases and result in more symmetrical peaks for both polar and non-polar compounds [3]. Carbon nanotubes utilized within open tubular capillaries have proven to be a robust stationary phase stable to high temperatures and capable of separating mixtures of compounds with good resolution [2]. Previously, we reported a microfabricated GC (micro-GC) chip implementing a SWCNT stationary phase [1], whereby the SWCNTs were deposited through the lithographic patterning of the growth catalyst on a silicon wafer [7]. Stationary phases that can be grown within a microfabricated channel eliminate the potentially problematic coating methods that are used with polymer-based stationary phases [8,9].

While our previous report demonstrated that a SWCNT stationary phase could be readily incorporated in a on-chip resistively heated micro-GC chip, providing fast temperature programmed separations on the order of a few seconds [1], there was an observable shortcoming in the uniformity of the SWCNT phase that appeared to limit the separation efficiency,  $N$ , and hence limit device performance. In order to address this shortcoming, a new growth recipe for producing a highly uniform SWCNT phase material has been implemented. This new growth recipe has been combined with a more effective bonding technique in order to prevent damage to the nanotubes during the bonding technique and reduce the amount of active glass surface. The channel structure is

30 cm in length, with a 50  $\mu\text{m}$  by 50  $\mu\text{m}$  cross-section., that in principle should be able to provide rapid and efficient GC separations [10,11]. Only one of the four walls is coated with the SWCNT stationary phase, a coating procedure that greatly simplifies the separation channel design. However, analyte mass transfer should be extremely rapid across the narrow channel, which should minimize the potential source of band broadening due to coating only one channel wall. Therefore, reduced plate height,  $h$ , measurements are reported and compared to the prior report in order to provide supporting evidence that the narrow channel cross-section with a uniform SWCNT phase does indeed provide improved performance. Additionally, the SWCNT stationary phase was characterized via SEM and Raman spectroscopy in order to verify the presence and quality of the SWCNTs in the channel and to determine the diameter of the nanotubes. The separations obtained with this micro-GC chip contain peaks with more Gaussian-like peak profiles, as will be demonstrated via peak symmetry measurements [12]. The on-chip resistive heater that incorporated a thin serpentine film of metal (5 nm of Ti and 100 nm of Pt) will also be shown to be significantly more efficient (improved relative to our initial report [1]).

## **2. Experimental**

### *2.1 Column Fabrication*

In brief, the separation channel and connecting ports were etched in a silicon wafer and the nanotubes were grown in the separation channel; the channel was then sealed with SU8 2005, thus producing the GC column. The serpentine resistive heating element was fabricated on the opposite side of the wafer.

Specifically, the fabrication process began with PR4640 photoresist (Shipley Company, Marlborough, MA, USA) spun on the back side of a 500  $\mu\text{m}$ -thick Si wafer with native oxide. Ports 380  $\mu\text{m}$  in circumference were patterned lithographically on the back of the wafer, then the photoresist was used as an etch mask for a 460  $\mu\text{m}$   $\pm$  10  $\mu\text{m}$  deep reactive ion etch (DRIE). After the etching process, the photoresist was removed from the back of the wafer. Next, PR4640 was again spun on the back side of the wafer and resistive heaters (metal film) were patterned onto the wafer, i.e., a 5 nm of Ti and 100 nm of Pt metal film was evaporated onto the wafer before the photoresist was removed again. Then, the front side of the wafer was coated with PR4620, and a 30 cm long and 50  $\mu\text{m}$  wide channel was patterned onto the wafer. The front channel was etched with DRIE to a depth of nominally 50  $\mu\text{m}$ , again using the photoresist as an etch mask. The resulting separation channel was 30 cm long with a 50  $\mu\text{m}$  x 50  $\mu\text{m}$  cross-section. The catalyst metals (100  $\text{\AA}$  Al, 1  $\text{\AA}$  Pt, 5  $\text{\AA}$  Fe) were deposited with an electron-beam evaporator, and lift-off was performed by soaking the wafer in acetone for 10 min, followed by brief (1-5 s) sonication and rinsing with acetone, ethanol and water.

The SWCNTs were grown onto one of the four walls of the separation channel via chemical vapor deposition. The 2 inch diameter furnace was heated to 500  $^{\circ}\text{C}$  before the wafer was introduced. The wafer was heated at a rate of 40  $^{\circ}\text{C}/\text{min}$  to 850  $^{\circ}\text{C}$  while flowing Ar gas at 240 ml/min combined with  $\text{H}_2$  at 160 ml/min. Once 850  $^{\circ}\text{C}$  were reached, the temperature was held constant until the end of the growth. After 10 min of heating, water was added to the reaction mixture by mixing argon that was bubbled through a water bubbler into the gas stream, maintaining the total flow of argon at 240 ml/min. The water content was regulated to be constant at 1000 ppm at the feed end.

After 20 min of heating, 40 ml/min of ethylene was added for 10 min (all gases in this process were from Matheson Tri-Gas, Newark, NJ, USA). During the growth, the pressure at the exhaust was maintained at 14 psi (99,300 Pa). The SWCNT coverage (i.e., on one wall of the separation channel) was analyzed with scanning electron microscopy (SEM).

After the growth of the SWCNT phase, the channel structure was sealed by spin-coating the glass cover slide with SU8 2005 (Micro Chem, Newton, MA, USA) at 500 rpm for 5 s, then 2000 rpm for 30 s. The glass slide was desiccated for 5 min at 200 °C then cooled by blowing nitrogen over it before the SU8 was added. The silicon column was firmly pressed on top of the coated glass slide, making sure there were no voids between the glass and the silicon. With the glass facing down, the wafer was baked in an oven by ramping to 65 °C at a rate of 5 °C/min and baking for 10 min, then ramping to 95 °C at 5 °C/min, baking for another 5 min, and finally ramping to 200 °C at 5 °C/min and baking for an additional 5 min.

## *2.2 Chromatographic Instrumentation*

All chromatographic experiments were completed using a Agilent 6890 GC (Agilent Technologies, Santa Clara, CA, USA) modified with a single diaphragm valve (Vici Valco, Houston, TX, USA) for high-speed sample injections onto the micro-GC chip, as previously reported [13-16]. The Agilent 6890 GC serves as a platform to study the separation performance of the micro-GC chip. Briefly, a sample is injected using the standard 6890 autoinjector, and a small portion of the autoinjected pulse is subsequently injected using the high-speed diaphragm valve (set to inject a 15 ms sample pulse for this study). This 15 ms sample pulse is then separated by the micro-GC chip with the



SWCNT stationary phase (either with or without on-chip resistive heating), followed by a high-speed FID. Note that the GC oven was used for the initial temperature setting, i.e., for isothermal separations as well. The timing and actuation of the diaphragm valve was controlled using an in-house written LabVIEW (National Instruments, Austin, TX) program [11] and the FID was modified with an in-house built electrometer for high-speed detection of the narrow chromatographic peaks (20,000 Hz sampling rate). All temperature programming was completed using the on-chip resistive heating element (discussed in more detail in section 2.1). The timing for the resistive heating was controlled via an in-house written LabVIEW program as previously reported [1,17]. A variable autotransformer (Stace Energy Products Co., Dayton, OH, USA) supplied a variable AC voltage (0 to 120 V) in order to resistively heat the micro-GC chip, as previously reported [1].

## *2.2 Chromatographic Experiments*

All chromatograms were collected with the 6890 GC inlet and FID temperature of 250 °C. The inlet was set for a splitless injection with a pressure of 10 psi (69,000 Pa) of hydrogen carrier gas, resulting in a carrier gas velocity of 95 cm/s at 50 °C. The transfer line from the 6890 GC autoinjector to the diaphragm valve was a 12 cm length of methyl deactivated capillary with an internal diameter of 100  $\mu\text{m}$ . The auxiliary pressure (for the hydrogen carrier gas through the chip) was also set at 10 psi (69,000 Pa). The micro-GC chip was interfaced to the diaphragm valve and FID with 13 and 16 cm lengths of methyl deactivated capillary, respectively, both with an internal diameter of 100  $\mu\text{m}$ . The capillary leads were attached to the micro-GC chip with high temperature epoxy (J-B

Weld, Sulfur Springs, TX, USA) as previously reported [1]. All chromatograms were obtained using a 15 ms injection pulse from the diaphragm valve.

### 3. Results and Discussion

#### 3.1 Characterization of the SWCNT stationary phase.

The SWCNT stationary phase on the one wall of the separation channel was characterized via both scanning electron microscopy (SEM) and Raman spectroscopy. The SEM images are shown in Figure 1. Note that while this characterization is described first for clarity, the experiments themselves were done last, after all the chromatographic experiments were completed, since the chip needed to be carefully sliced open orthogonal to the channel to facilitate SEM and Raman characterization. Several channel locations were examined, and the results presented are representative and consistent.

The image in Figure 1 is a SEM image and shows that the nanotubes have formed a relatively uniform mat in the microfabricated channel. This is different than the tangles (with voids) of SWCNTs that were previously reported [1]. The image in Figure 1 shows that the SWCNTs are  $\sim 800$  nm tall within the channel. The SWCNT stationary phase was further characterized utilizing Raman spectroscopy. The full spectrum is shown in Figure 2A; the presence of the narrow G-band ( $1500\text{-}1700\text{ cm}^{-1}$ ) suggests the presence of SWCNTs within the channel. The large intensity of the broad D-band ( $1250\text{-}1400\text{ cm}^{-1}$ ), however, suggests that there may be some defects present such as shortened tubes, vacancies and/or multi-wall carbon nanotubes [18]. The ring breathing modes ( $< 500\text{ cm}^{-1}$ ), shown in Figure 2B, suggest the presence of SWCNTs with a diameter of  $\sim 2$  nm

[18]. Overall, the SWCNT stationary phase appears reasonably uniform in size and distribution on the one wall within the micro-GC channel. Other channel locations analyzed provided similar results, not shown for brevity.

### *3.2 On-chip resistive heating as a means of temperature programming.*

The micro-GC chip with SWCNT stationary phase was utilized to separate a mixture of five *n*-alkanes (*n*-hexane, *n*-octane, *n*-nonane, *n*-decane and *n*-undecane). The isothermal separation of the mixture at 50 °C is shown in Figure 3A. The separation is complete in less than 10 s with the earlier peaks eluting with good signal-to-noise and adequate resolution. The later eluting peaks (*n*-decane and *n*-undecane) have significantly larger peak widths, and *n*-undecane is barely visible above the baseline. An increase of the isothermal temperature to 100 °C resulted in the separation shown in Figure 3B. The separation is complete in less than 2 s, which is 5-fold faster than the isothermal separation at 50 °C (Figure 3A); however, the earlier eluting peaks are overlapped significantly. The decreased peak widths of the later eluting peaks and the increased signal-to-noise for *n*-undecane demonstrate the benefit of the higher isothermal temperature (100 °C). This is commonly referred to as the general elution problem, where for GC no single isothermal temperature provides optimal resolution with consistently narrow peaks for a mixture of compounds with a sufficiently wide boiling point range.

A common solution to the general elution problem is the use of temperature programming. To address this issue, this micro-GC chip was equipped with an on-chip resistive heating element. Applying a voltage across the heating element results in a rapid and reproducible temperature program [1]. The five compound *n*-alkane mixture

separated isothermally in Figures 3A and 3B was temperature programmed by applying 36 V to the heating element, producing a temperature program of 26 °C/s (with the calibration of the programming rate described in section 3.3). The resulting temperature programmed separation is shown in Figure 3C. The separation is complete in less than 2.5 s with sufficient resolution between all of the analytes and an improved signal-to-noise ratio for *n*-undecane, when compared to the separation obtained at an isothermal temperature of 50 °C. A plot of the peak width-at-half-height,  $w_h$ , as a function of the adjusted retention time,  $t_R - t_M$  (the retention time minus the dead time), for both the isothermal (at 50 °C) and temperature programmed separation is shown in Figure 3D. Temperature programming significantly reduces the width and retention time of the more retained compounds, which leads to a larger S/N ratio. For example, at a common adjusted retention time of  $\sim 0.9$  s, the temperature programmed peak width is approximately half of the isothermal peak width.

### 3.3 Calibration of the temperature programming rate.

The new micro-GC chip was characterized isothermally using a single analyte to determine the linearity of analyte retention as a function of temperature, and ultimately to calibrate the temperature programming rate as a function of applied voltage. The test analyte, *n*-decane, was injected at four isothermal temperatures in order to create a van't Hoff plot (a plot of  $\ln k$  vs.  $1/T$ ). This plot along with the best fit line and equation are shown in Figure 4. The equation of the line shown was used, as previously reported [1,17], to determine the rate of temperature programming. The rates of temperature programming resulting from several different voltages are tabulated in Table 1. The linearity of the van't Hoff plot suggests that the low temperatures do not adversely affect

the retention of the analyte; the retention of *n*-decane is linear over the temperature range reported. Also, the on-chip resistive heater employed appears to be slightly more efficient than the previously reported model [1]. The previously reported temperature program of 60 °C/s was produced by applying 96 V to the heating element. The new micro-GC chip would require one third less voltage (63 V as extrapolated from the data in Table 1) to produce the same temperature programming rate.

### *3.4 Comparison of the new SWCNT micro-GC chip to previous study*

The SWCNT micro-GC chip reported herein is a redesign and improvement over our previous report [1] (see p. 5642, Figure 4B and p. 5643 Table 1 of that reference), consequently a comprehensive comparison of the two chips is presented. The previously reported chips resulted in chromatograms with moderately tailing peaks (even when temperature programmed). Chromatograms obtained with the chips reported herein contain peaks that are significantly more Gaussian-like in nature. The peak tailing, even in the isothermal chromatogram at 50 °C, is minimal when compared to the previously reported chips. The separations using the new chips resulted in a 66 % reduction in the skew of the isothermal *n*-hexane peaks. For *n*-octane, which was slightly more retained, a reduction in the skew of 98 % was observed.

Another significant difference between the previously reported micro-GC chip and the new micro-GC chip relates to band broadening, which can be objectively compared via reduced plate height,  $h$ , values. Data for the purpose of comparing band broadening performance is presented in Figure 5. A plot of the width-at-half-height,  $w_h$ , as a function of the adjusted retention time,  $t_R - t_M$ , for the previously reported micro-GC chip and new micro-GC chip is shown in Figure 5A, for isothermal separations.

Similarly, in Figure 5B are the data for both micro-GC chips using temperature programming. The data in Figure 5A will allow for a comparison of the isothermal separations for the two micro-GC chips. For isothermal GC, band broadening is essentially linear with adjusted retention time (as well as  $k$ ) [11]. The plot in Figure 5B will allow for a comparison of the temperature-programmed separations for the two micro-GC chips. The analyte *n*-hexane, with the smallest adjusted retention time on the previously reported micro-GC chip, has a peak width that is actually 4-fold narrower than obtained with the new chip, ~12 ms versus ~50 ms. This is predominately due to the difference in the carrier gas velocities for the two chips. The previous micro-GC chip was operated at an average linear flow velocity,  $\bar{u}$ , of ~1100 cm/s while the new micro-GC chip was operated at a  $\bar{u}$  of ~95 cm/s. Meanwhile, as for the more retained analytes, the peak widths on the new chip are significantly narrower. However, peak widths directly can not be used to compare separation performance; for that purpose one must put the band broadening data on a common field of comparison, that is, by use of reduced plate height calculations.

In order to make a quantitative comparison between the previous and new micro-GC chips, the data presented in Figure 5A can be used to calculate the reduced plate height,  $h$ . The determination of separation efficiency is often reported as  $N$ ,

$$N = 5.545 \left( \frac{t_R}{w_h} \right)^2 \quad (1)$$

Using the efficiency calculated in Eq. (1), and the length of the separation channel,  $L$ , the plate resulting plate height,  $H$ , can be calculated using the following equation:

$$H = \frac{L}{N} \quad (2)$$

To remove the dependence of  $H$  on the dimensions of the separation channels the reduced plate height,  $h$ , can be calculated,

$$h = \frac{H}{d} \quad (3)$$

where  $d$  is the width of the separation channel. For the previous micro-GC chip  $d = 100 \mu\text{m}$  and for the new micro-GC chip  $d = 50 \mu\text{m}$ . It is important to note that  $h$  is independent of the dimensions of the separation channel. A plot of  $h$  as a function of the retention factor,  $k$ , for the isothermal data from Figure 5A is shown in Figure 5C, where  $k$  is equal to  $(t_R - t_M) / t_M$ . The test analyte *n*-hexane is essentially unretained, therefore the  $h$  values for *n*-hexane for each chip can be compared to objectively determine the differences in applied linear flow velocity (not being optimum in either case), and differences in extra-column band broadening. When  $k$  is approximately equal to zero, which is the case for an *n*-hexane,  $h$  for the previous micro-GC chip is  $\sim 16$  while  $h$  for the new micro-GC chip is  $\sim 4$ . This implies a 4-fold reduction of  $h$  when comparing the previous and new micro-GC chips, while not taking into account any improvement in the new micro-GC chip due to the stationary phase. For analytes that are retained significantly by the SWCNT stationary phase the same comparison of  $h$  can be made, and ultimately corrected for  $h$  improvement of an unretained analyte, to determine the improvement factor due to the refined SWCNT stationary phase. For an analyte retained on the previous chip,  $h$  is  $\sim 200$ , based on the average  $h$  for the three retained analytes for the previous chip in Figure 5C, where  $h$  is essentially leveled off (constant). Using the new chip, a retained analyte results in an  $h$  of  $\sim 10$ , using the average of the three most retained analytes in Figure 5C. Therefore, for a retained analyte the new chip provides a 20-fold reduction in  $h$ . Consequently, correcting by the 4-fold difference in  $h$  for the

unretained analyte, a 5-fold reduction in  $h$  due to the improvements to the stationary phase morphology and uniformity was achieved.

The new micro-GC chip has a separation channel that is 30 cm with a 50  $\mu\text{m}$  x 50  $\mu\text{m}$  cross-section. The previously reported micro-GC chip had a separation channel 50 cm in length with a 100  $\mu\text{m}$  x 100  $\mu\text{m}$  cross-section. The dependence on channel dimensions for the anticipated peak width, in the absence of any extra-column band broadening, can be estimated from Golay theory [11]. The additional 5-fold decrease in  $h$  (beyond the 4-fold decrease in  $h$  for an unretained analyte) for the new micro-GC chip is a combination of factors. These factors include, but are not limited to, the new nanotube growth recipe that led to a uniform thickness of the nanotube “mat” in the channel (per Figure 1), the uniform size of the nanotubes (length and diameter), and the different chip bonding technique. The major improvements in peak shape and reduction in  $h$  suggest that the presented micro-GC chip utilizing SWCNTs as the stationary phase is a significant enhancement of the previously reported chips.

#### **4. Conclusions**

The micro-GC chip reported herein utilized a single-wall carbon nanotube (SWCNT) stationary phase grown utilizing a new growth recipe, which resulted in an improvement in peak symmetry, a reduction of the reduced plate height, and hence an improvement in separation efficiency. Micro-GC chips can be fabricated in a batch format because multiple columns can be etched onto one wafer. The lower energy and carrier gas consumption make these chips more appealing and likely more applicable for field portable applications of micro-GC.



## Acknowledgements:

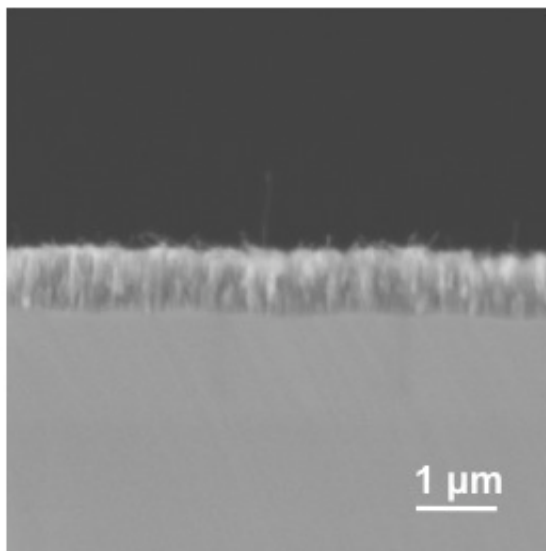
This work was supported by the DARPA MGA program and performed under the auspices of the U.S. Department of Energy by Lawrence Livermore National Laboratory under Contract DE-AC52-07NA27344. MS and OB would like to acknowledge the DARPA MGA program for funding.

## References

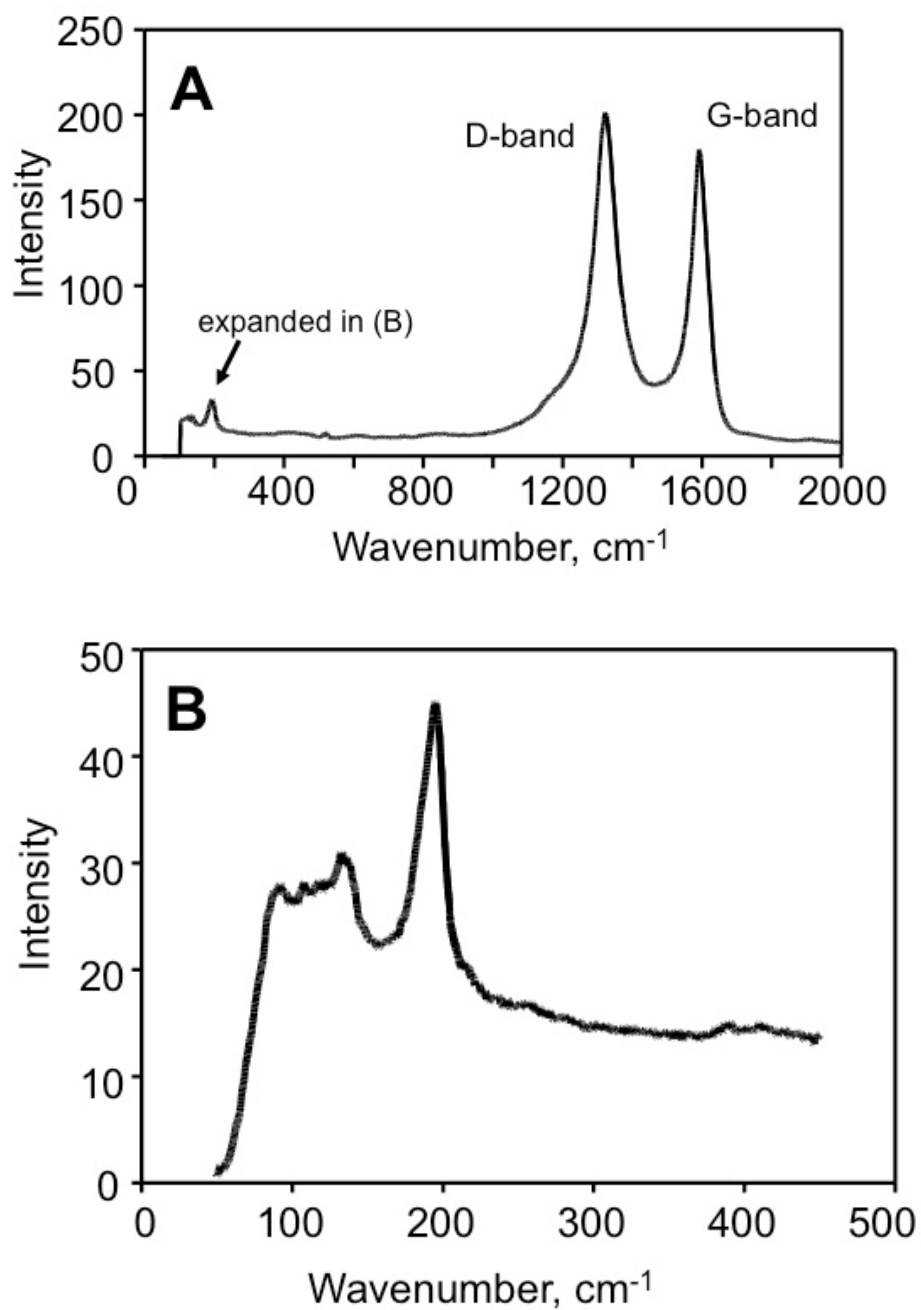
- [1] M. Stadermann, A.D. McBrady, B. Dick, V.R. Reid, A. Noy, R.E. Synovec, O. Bakajin, *Anal. Chem.* 78 (2006) 5639.
- [2] C. Saridara, S. Mitra, *Anal. Chem.* 77 (2005) 7094.
- [3] Q. Li, D. Yuan, *J. Chromatogr. A* 1003 (2003) 203.
- [4] L.A. Kartsova, A.A. Makarov, *J. Anal. Chem.* 59 (2004) 724.
- [5] L. Yuan, C. Ren, L. Li, P. Ai, Z. Yan, M. Zi, Z. Li, *Anal. Chem.* 78 (2006) 6384.
- [6] L.A. Kartsova, A.A. Markov, *Russ. J. Appl. Chem.* 75 (2002) 1725.
- [7] J. Kong, H.T. Soh, A.M. Cassell, C.F. Quate, H. Dai, *Nature* 395 (1998) 878.
- [8] K. Grob, *Making and Manipulating Capillary Columns for Gas Chromatography*, Verlag, Heidelberg, 1986.
- [9] G.M. Gross, J.W. Grate, R.E. Synovec, *J. Chromatogr. A* 1029 (2004) 185.
- [10] V.R. Reid, R.E. Synovec, *Talanta*, (2008), doi:10.1016/j.talanta.2008.05.012.
- [11] G.M. Gross, B.J. Prazen, J.W. Grate, R.E. Synovec, *Anal. Chem.* 76 (2004) 3517.
- [12] J.P. Foley, J.G. Dorsey, *Anal. Chem.* 55 (1983) 730.
- [13] J.L. Hope, K.J. Johnson, M.A. Cavelti, B.J. Prazen, J.W. Grate, R.E. Synovec, *Anal. Chim. Acta* 490 (2003) 223.
- [14] C.A. Bruckner, B.J. Prazen, R.E. Synovec, *Anal. Chem.* 70 (1998) 2796.
- [15] C.G. Fraga, B.J. Prazen, R.E. Synovec, *Anal. Chem.* 72 (2000) 4154.
- [16] A.E. Sinha, K.J. Johnson, B.J. Prazen, S.B. Lucas, C.G. Fraga, R.E. Synovec, *J. Chromatogr. A* 983 (2003) 195.
- [17] V.R. Reid, A.D. McBrady, R.E. Synovec, *J. Chromatogr. A* 1148 (2007) 236.
- [18] A.C. Dillion, M. Yudasaka, M.S. Dresselhaus, *J. Nanosci. Nanotech.* 4 (2004) 691.



## Figure Captions

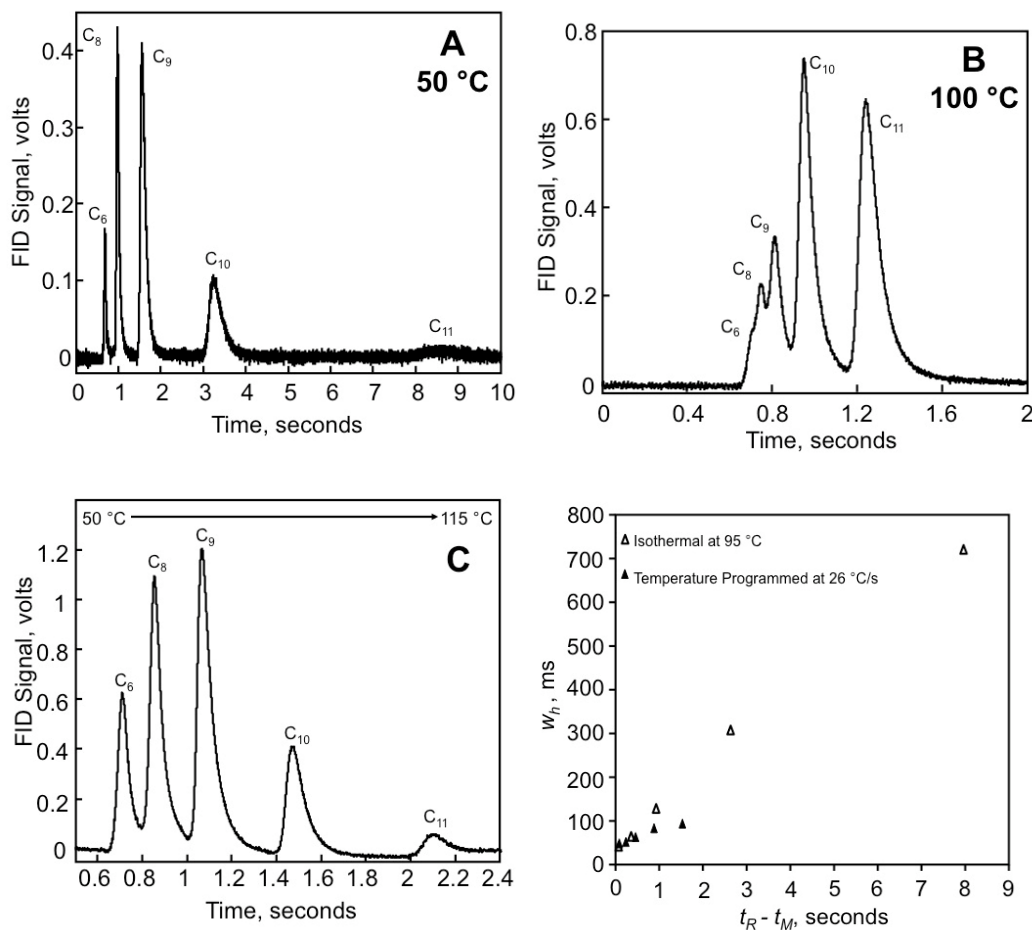


**Figure 1.** SEM image of the stationary phase composed of a “mat” of SWCNTs within a micro-GC separation channel.

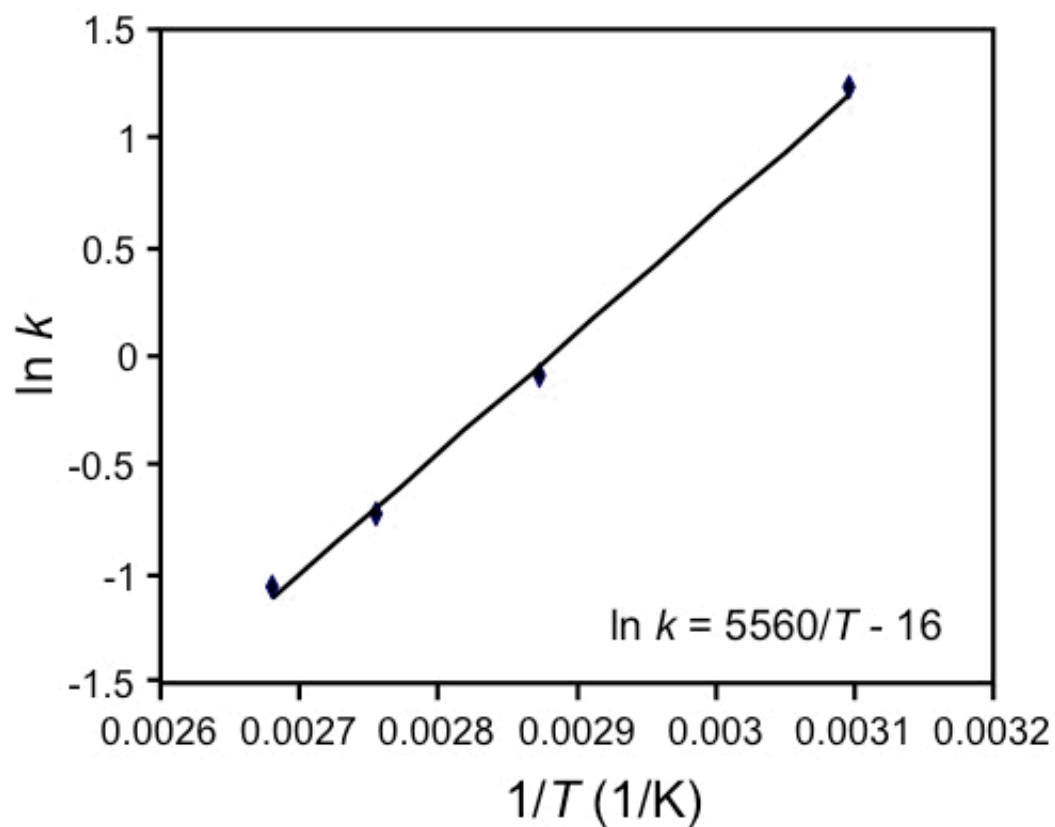


**Figure 2.**

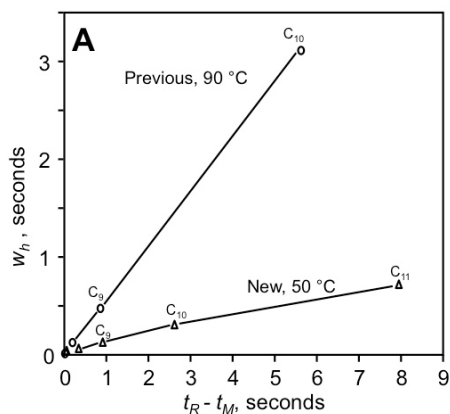
Raman spectra of the SWCNT stationary phase grown in the separation channel. (A) Raman spectrum showing both the D-Band ( $\sim 1350 \text{ cm}^{-1}$ ) and G-Band ( $\sim 1600 \text{ cm}^{-1}$ ). (B) Detail of the radial breathing modes ( $< 500 \text{ cm}^{-1}$ ) of the spectrum shown in (A).



**Figure 3.** Isothermal and temperature programmed separations of a five compound *n*-alkane mixture (retention order: *n*-hexane (C<sub>6</sub>), *n*-octane (C<sub>8</sub>), *n*-nonane (C<sub>9</sub>), *n*-decane (C<sub>10</sub>), *n*-undecane (C<sub>11</sub>)). All data collected using H<sub>2</sub> carrier gas at an absolute head pressure of 10 psi (69,000 Pa). Separations were obtained using the 30 cm micro-GC chip with a 50 μm x 50 μm channel cross-section. (A) Separation obtained at an isothermal temperature of 50 °C. (B) Separation obtained at an isothermal temperature of 100 °C. (C) Temperature programmed separation obtained by applying 60 volts across the on-chip resistive heating element resulting in a temperature programming rate of 26 °C/sec (initial column temperature was 50 °C). (D) A plot of width-at-half-height,  $w_h$ , as a function of adjusted retention time,  $t_R - t_M$ , for the separations in (A) and (C). Methane was the dead time marker,  $t_M = 632$  ms.



**Figure 4.** Van't Hoff plot ( $\ln k$  vs.  $1/T$ ) of  $n$ -decane for the micro-GC chip with the SWCNT stationary phase used for the calibration of the temperature programming rates. The best fit line and equation are displayed on the graph. All data obtained using  $H_2$  carrier gas at an absolute head pressure of 10 psi (69,000 Pa). Methane was used as a dead time marker for  $k$  calculations.



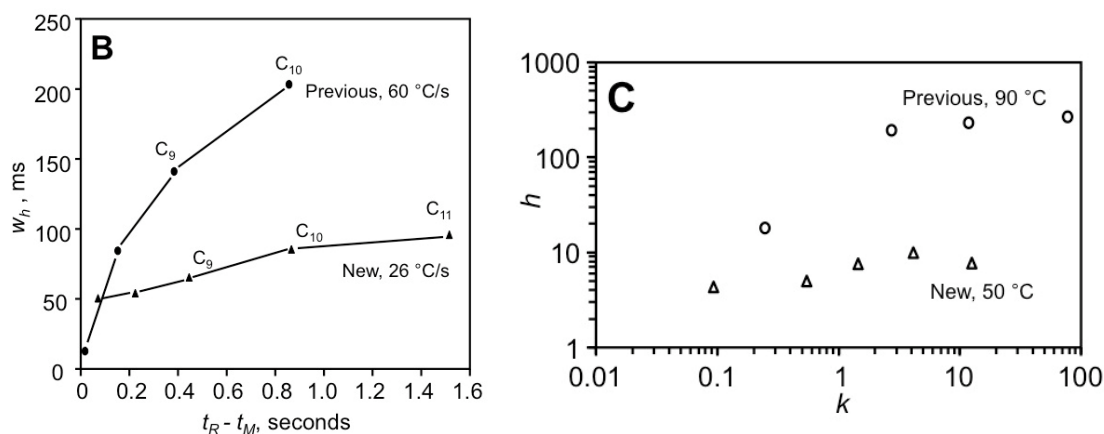


**Figure 5.** Comparison of previously published [1] and current (new) generation SWCNT micro-GC chips. A plot of width-at-half-height,  $w_h$ , as a function of adjusted retention time,  $t_R - t_M$ , for the previous and new chips. The previously reported data consists of data for four different analytes: *n*-hexane, *n*-octane, *n*-nonane ( $C_9$ ), and *n*-decane ( $C_{10}$ ). The new generation chip data consists of data for five different analytes: *n*-hexane, *n*-octane, *n*-nonane, *n*-decane and *n*-undecane ( $C_9$ ,  $C_{10}$  and  $C_{11}$  labeled as in Figure 3). (A) Isothermal data for both generations of SWCNT micro-GC chips. Previously reported isothermal data collected at 90 °C ( $\circ$ ) where  $t_M = 73$  ms, new chip isothermal data collected at 50 °C ( $\Delta$ ) where  $t_M = 632$  ms. (B) Temperature programmed data for both generations of chips, with previous data collected at a program rate of 60 °C/s ( $\bullet$ ) where  $t_M = 73$  ms and new chip collected at a temperature rate of 26 °C/s ( $\blacktriangle$ ) where  $t_M = 632$  ms. (C) A plot of reduced plate height,  $h$ , as a function of retention factor,  $k$ , for the isothermal data for both generations of SWCNT micro-GC chips. Previously reported isothermal data collected at 90 °C ( $\circ$ ) where  $t_M = 73$  ms, new chip isothermal data collected at 50 °C ( $\Delta$ ) where  $t_M = 632$  ms.

Table 1. Temperature programming rates for the on-chip resistive heater ( $T_i = 50\text{ }^{\circ}\text{C}$ ) for various applied voltages.

Voltage Applied (V)	Temperature Programming Rate ( $^{\circ}\text{C/s}$ )
24	10
30	18
36	26
42	33